

Supplementary data

Multifunctional polyurethanes synthesized from different triarylamine units for electrochromic, photogenerated, resistance memory, sensor devices

Xu Zhang^a, Qingyi Lu^a, Caiyu Yang^a, Shuo Zhao^a, Yan Wang^a, Wei Zhang^a, Haijun

Niu^{a,*}, Ping Zhao^b, Wen Wang^{c,*}, and Jinghe Fan^a

^a Key Laboratory of Functional Inorganic Material Chemistry, Ministry of Education, Department of Macromolecular Science and Engineering, School of Chemical, Chemical Engineering and Materials, Heilongjiang University, Harbin 150080, P R China

^b Key Laboratory for Advanced Materials and Institute of Fine Chemicals, East China University of Science and Technology, Shanghai 20037, PR China.

^c School of Materials Science and Engineering, Harbin Institute of Technology, Harbin 150080, P R China

*Correspondence: haijunniu@hotmail.com; wangwen@hit.edu.cn

Materials and Measurements.

N,N'-diphenyl-1,4-phenylenediamine, N,N'-di-2-naphthyl-1,4-phenylenediamine, aniline, bis(trichloromethyl) carbonate, 4,4'-diphenylmethane diisocyanate (4,4'-MDI), dibutyltindilaurate (DBTDL), 4-fluoronitrobenzene, diamidhydrate ($\text{N}_2\text{H}_4 \cdot \text{H}_2\text{O}$), polyethylene glycol (PEG-2000), sodium hydride (NaH, Acros), calcium hydride (CaH), Palladium on matrix carbon powder (10wt.% loading), tetrabutylammonium perchlorate (TBAP) were used directly without any pretreatment (Aladdin). Nitrobenzene (NB), 4-nitrotoluene (NT), 2,4-dinitrotoluene (DNT), 4-nitrophenol (NP), 2,4-dinitrophenol (DNP) were purchased from Sigma Aldrich, 2,4,6-trinitrotoluene (TNT) and 2,4,6-Trinitrophenol (TNP) were obtained from Ultra Scientific. And all the solvents used in this report were purified by vacuum distillation (-0.1 MPa) after dried over CaH for a night.

Nuclear magnetic resonance (NMR) spectra were recorded on a Bruker spectrometer with Bruker AC-400 MHz in deuterate DMSO. The molecular weight information on PUs were determined on Gel permeation chromatography (GPC) unit equipped with double refractive index detector with DMF mixed with LiCl as an eluent at a flow rate of 1.0 mL/min. Thermogravimetric analysis (TGA) was conducted on a PerkinElmer TGA in the temperature range of 0–800 °C under nitrogen atmosphere with a heating rate of 10 K min⁻¹. The theoretical study was performed on the 6-31G basis set in Gaussian09 using the density functional theory (DFT), as approximated by the B3LYP.

Cyclic voltammograms of the PUs were conducted on CH Instruments 660A Electrochemical Workstation (Shanghai, China) with 0.1 mol/L electrolyte (the mixture of TBAP and dry acetonitrile) at a scan rate of 50 mV s⁻¹. The conventional three-electrode cell was using an Ag/AgCl electrode worked as the reference electrode, a platinum (Pt) wire electrode worked as the counter electrode, and PUs/ Indium tin oxide (ITO) worked as the working electrode, respectively. UV-vis spectra were collected using UV-3600 spectrophotometer (Shimadzu). Photoluminescence (PL) spectra were performed by a

Jasco FP-6200 spectrometer. The I-V characterization curves were performed by a Keithley 4200-SCS semiconductor analyzer. The mechanical properties of these polymers were examined with Instron 3367 universal testing machine at room temperature.

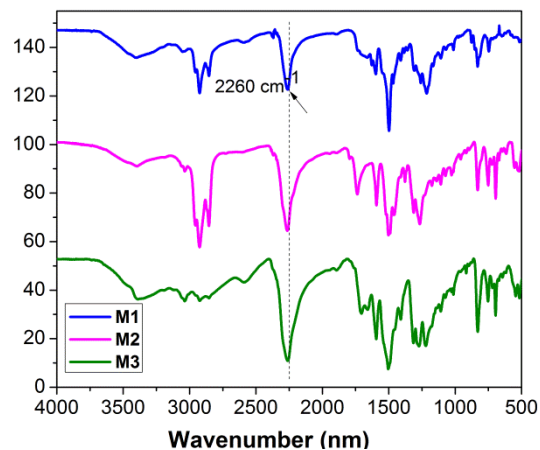
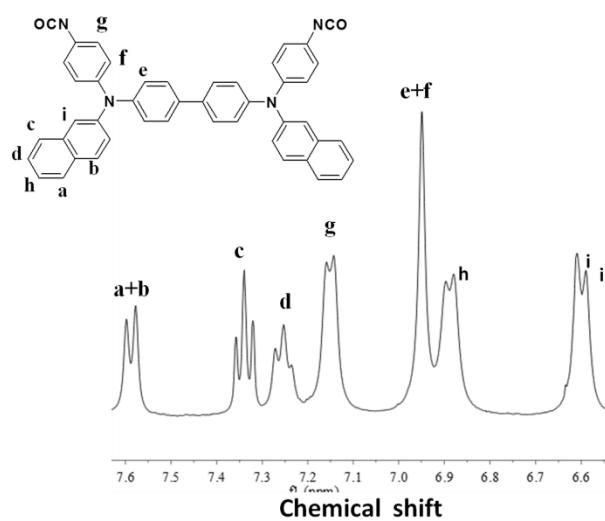


Fig. S1. FTIR spectra of three monomers.



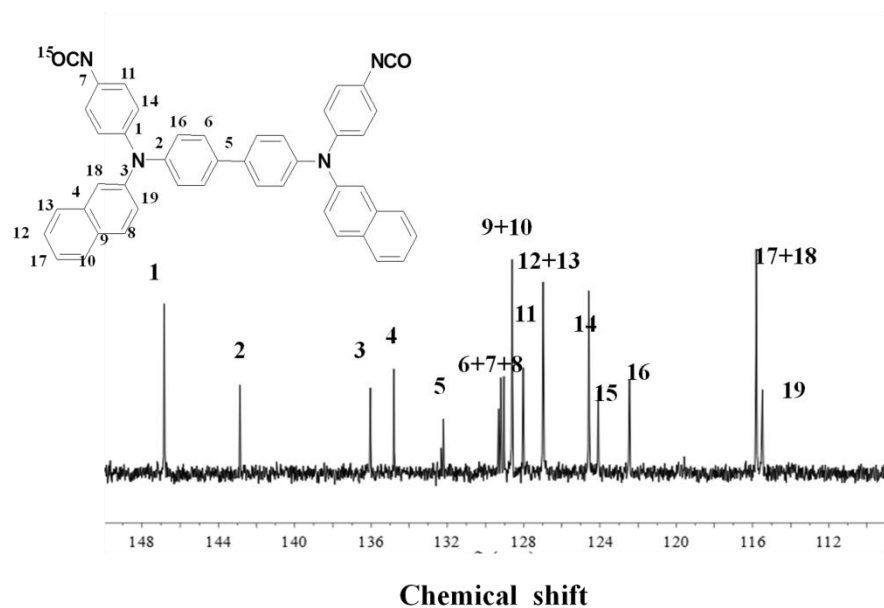
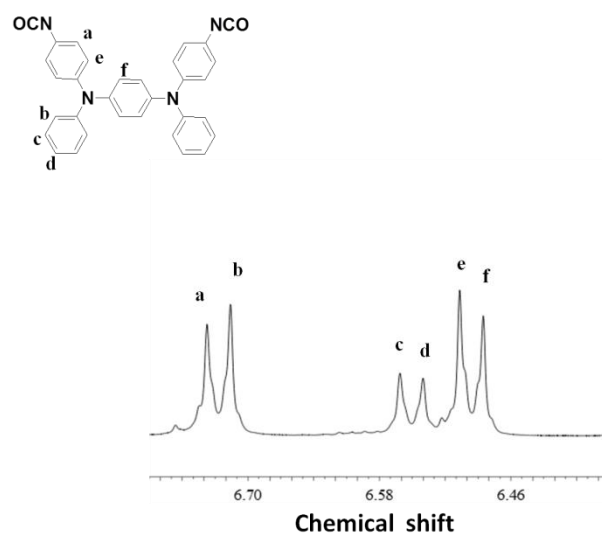


Fig. S2. (a) ^1H NMR; (b) ^{13}C NMR spectra of **M1** in $\text{DMSO}-d_6$.



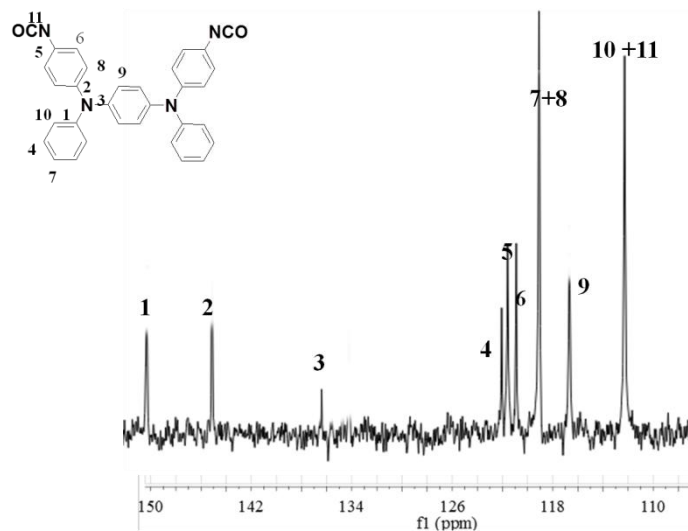


Fig. S3. (a) ^1H NMR; (b) ^{13}C NMR spectra of **M2** in $\text{DMSO-}d_6$.

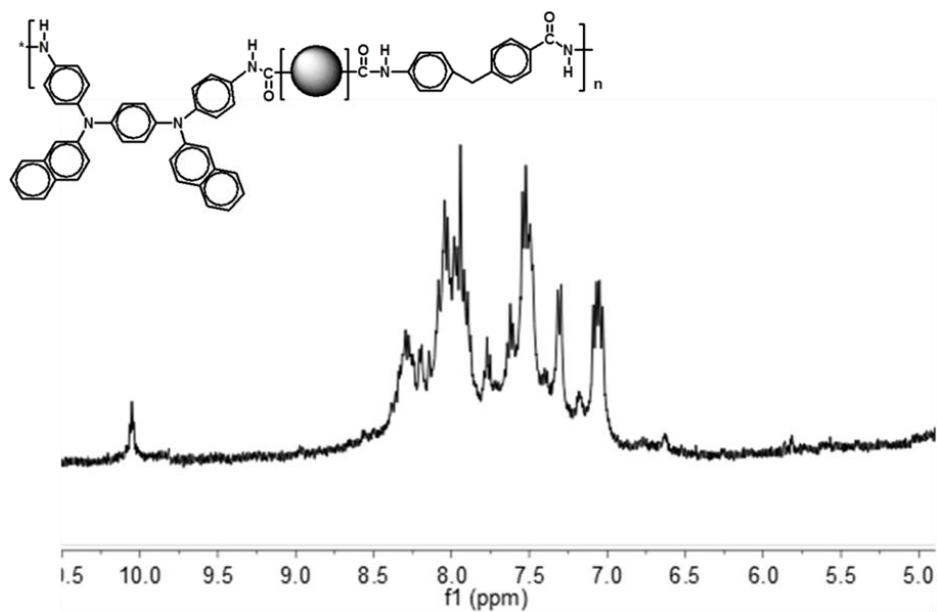


Fig. S4. ^1H NMR spectrum of **PU1** in $\text{DMSO-}d_6$

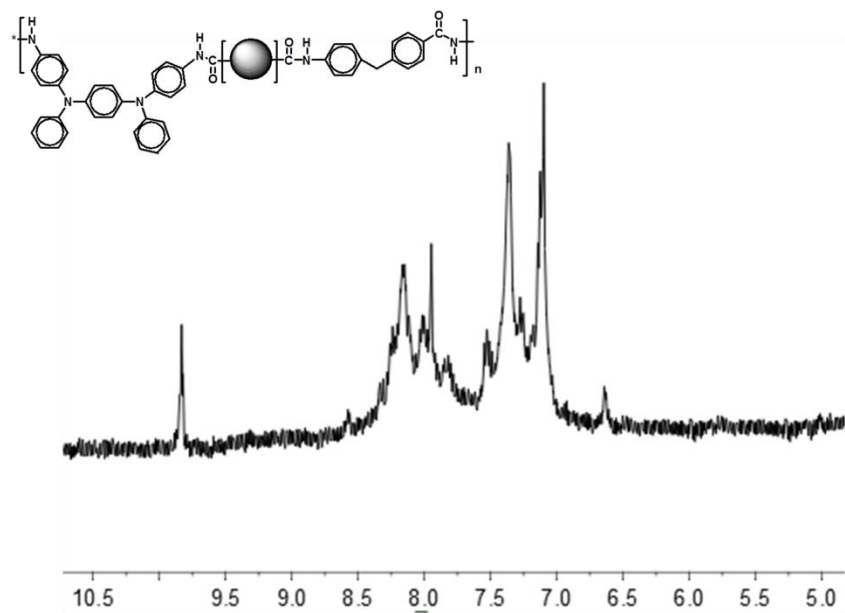


Fig. S5. ¹H NMR spectrum of PU2 in DMSO-*d*₆

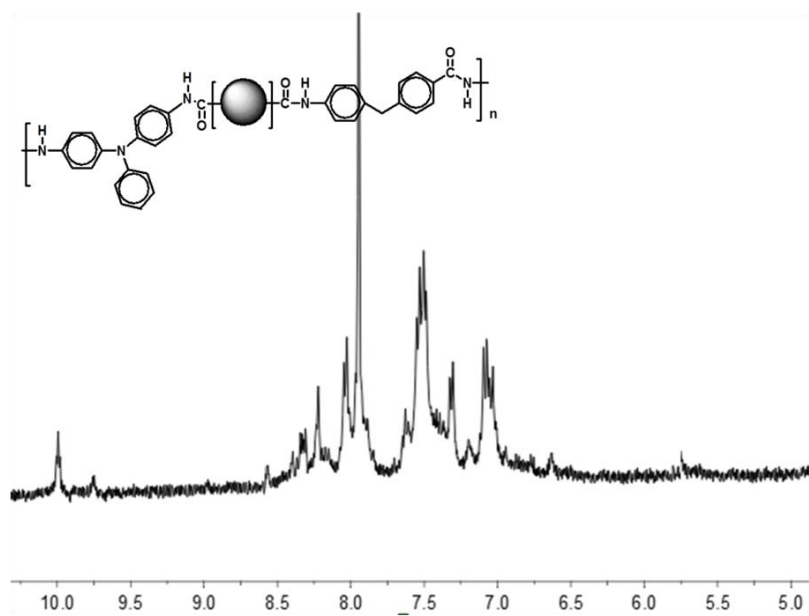


Fig. S6. ¹H NMR spectrum of PU3 in DMSO-*d*₆

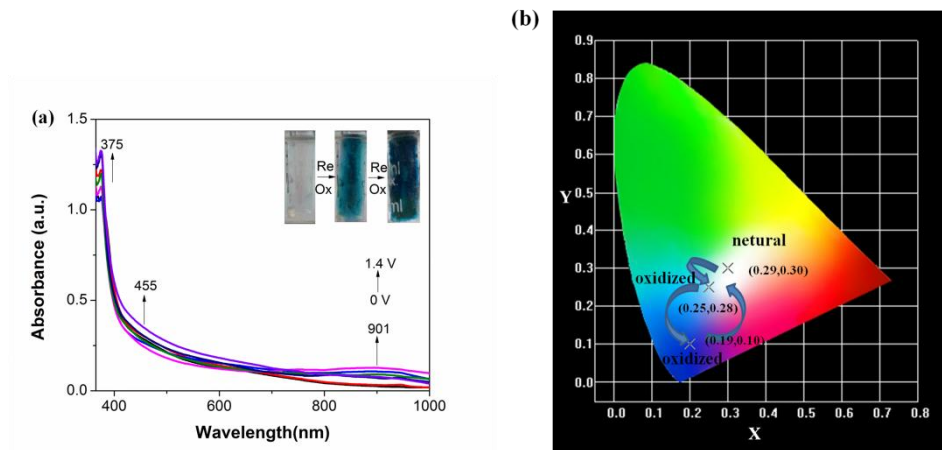


Fig. S7. Absorption spectra of the PU2 (a) at different applied potentials (0.0-1.4 V) and the color coordinates (b) of it. The insets of (a) showing the color changes.

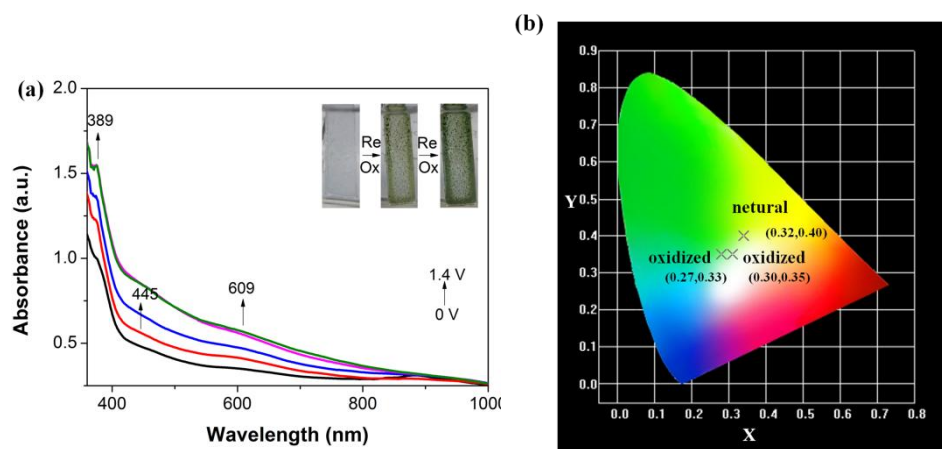


Fig. S8. Absorption spectra of the PU3 (a) at different applied potentials (0.0-1.4 V) and the color coordinates (b) of it. The insets of (a) showing the color changes.

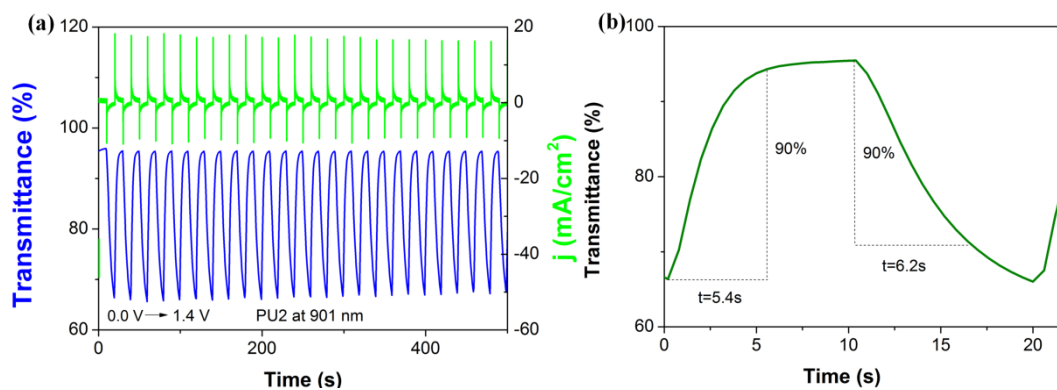


Fig. S9. (a) Optical switching the transmittance and current between 0.0 and 1.4 V of the PU2 with a cycle time of 10 s. (b) Optical switch time (monitored at 901 nm).

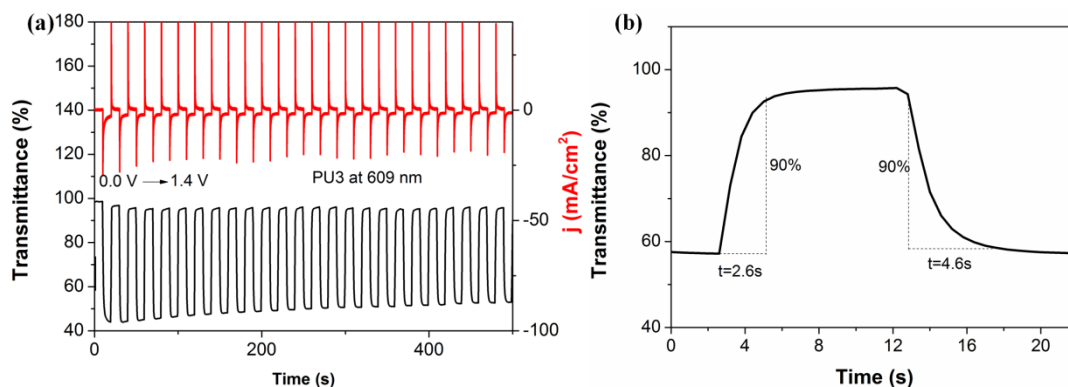


Fig. S10. (a) Optical switching the transmittance and current between 0.0 and 1.4 V of the PU3 with a cycle time of 10 s. (b) Optical switch time (monitored at 609 nm).

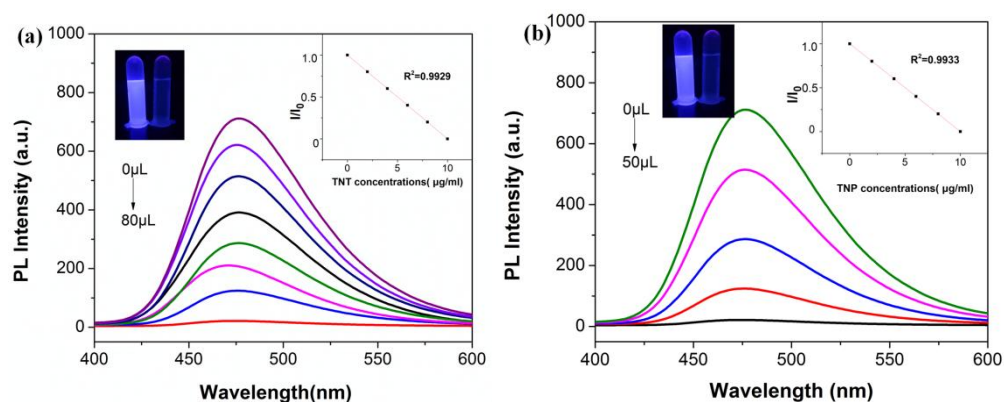


Fig. S11. Changes in fluorescence spectra of PU2 (1×10^{-5} M) upon addition of different concentration of (a) TNT (0 uL to 80 uL) and (c) TNP (0 uL to 50 uL) in NMP.

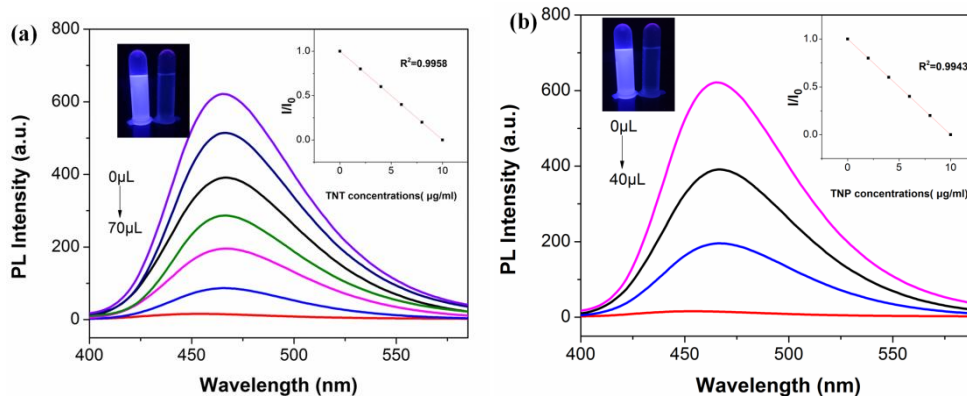


Fig. S12. Changes in fluorescence spectra of PU1 (1×10^{-5} M) upon addition of different concentration of (a) TNT (0 uL to 70 uL) and (c) TNP (0 uL to 40 uL) in NMP.

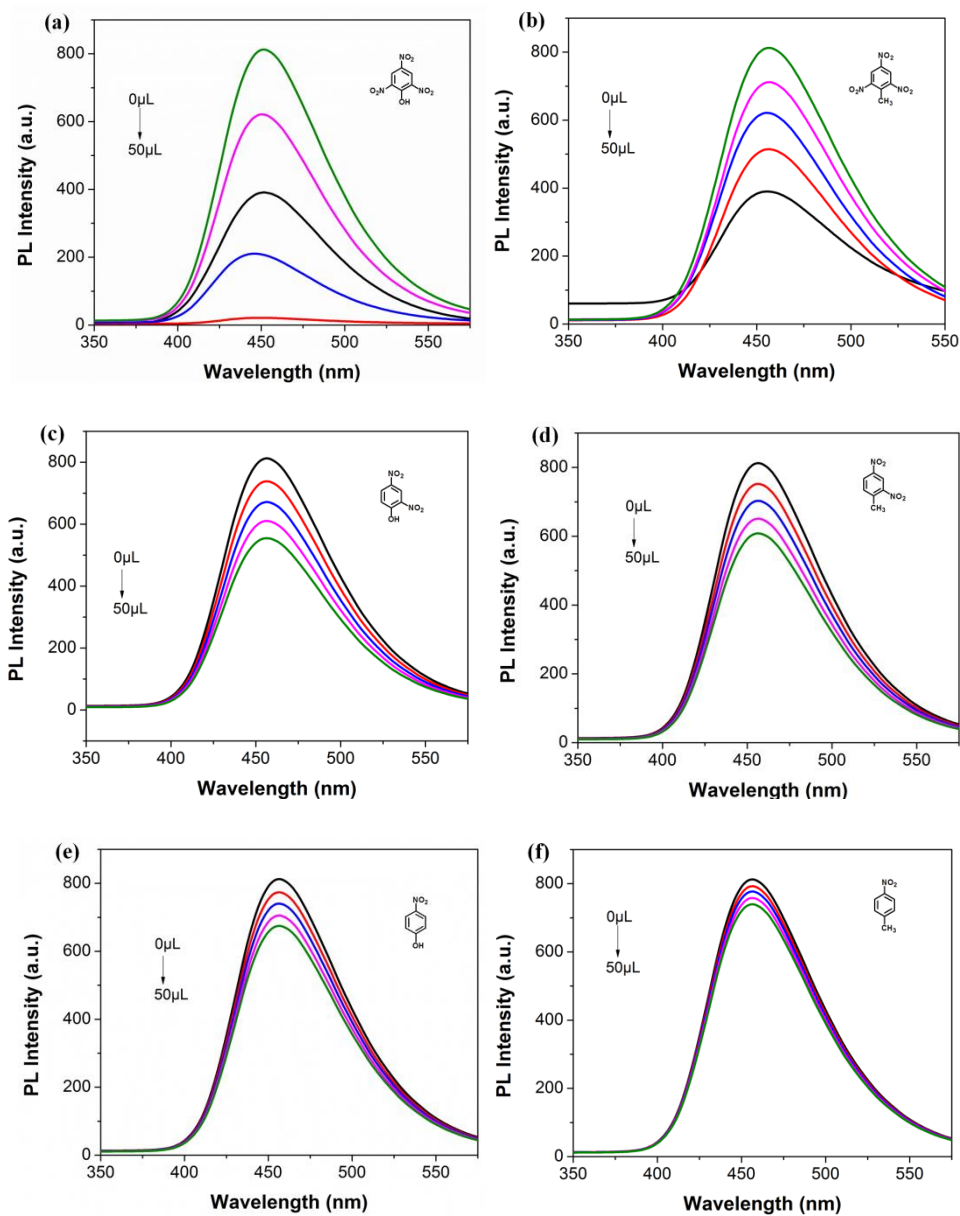


Fig. S13. Changes in fluorescence spectra of PU3 (1×10^{-5} M) upon addition of different concentration (0 μ L to 50 μ L) of (a) TNP, (b) TNT, (c) DNP, (d) DNT, (e) NP and (f) NT in NMP.

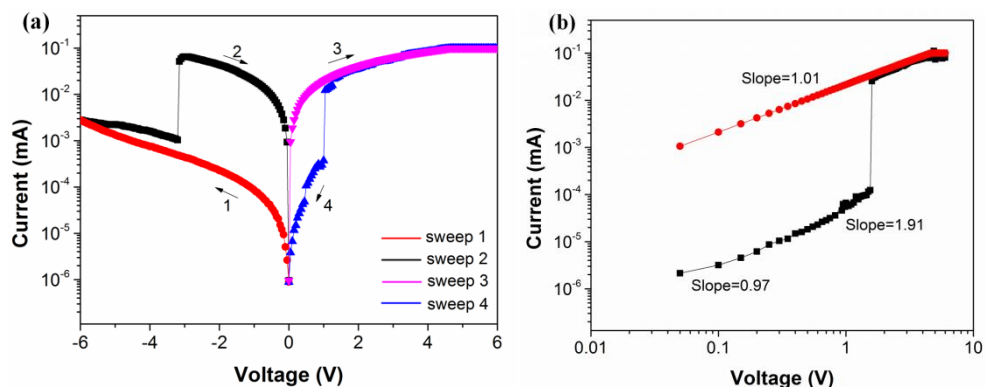


Fig. S14. (a) I-V curve and (b) Linear fitting and corresponding slopes of the memory device based on PU2.

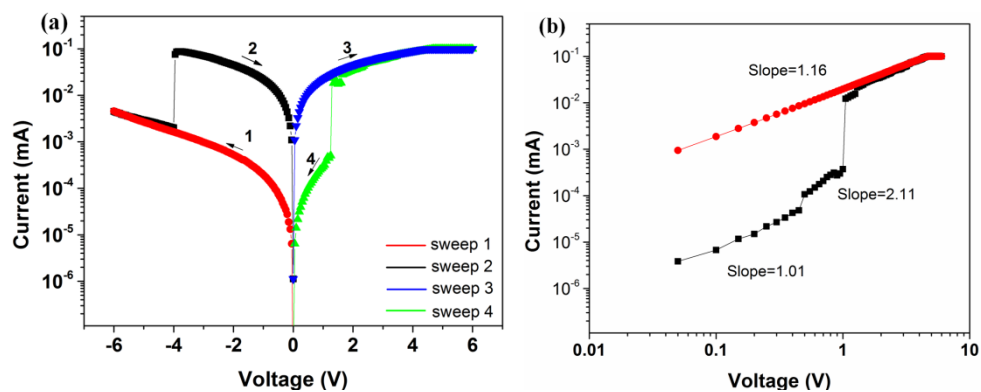


Fig. S15. (a) I-V curve and (b) Linear fitting and corresponding slopes of the memory device based on PU3.

Table S1. Optical properties of PUs.

PUs	In solution λ (nm) ^a			As film λ (nm)		
	abs max	PL max	Φ_{PL} (%) ^b	abs max	abs onset	PL max
PU1	369	465	13.1	377	432	476
PU2	378	477	20.8	375	422	481
PU3	381	455	35.1	389	477	465

^a PUs solutions in dilute NMP at a concentration of about 1×10^{-5} mol L⁻¹;

^b Measured by using quinine sulfate as a reference standard ($\Phi_{PL} = 54.6\%$).

Table S2. Electrochemical properties of PUs.

PU _s	$\lambda_{\text{onset}}^{\text{abs}}$ ^a	$E_{\text{onset}}^{\text{peak}}$ ^b	$E_{\text{HOMO}}^{\text{electro}}$ ^c	$E_{\text{LUMO}}^{\text{electro}}$ ^c	$E_{\text{g}}^{\text{film}}$ ^d	$E_{\text{HOMO}}^{\text{quntum}}$ ^e	$E_{\text{LUMO}}^{\text{quntum}}$ ^e	$E_{\text{g}}^{\text{quntum}}$ ^e
	vs Ag/AgCl							
PU1	432	0.29	-4.06	-1.19	2.87	-4.03	-0.92	3.11
PU2	477	0.43	-3.92	-1.32	2.60	-4.19	-1.22	2.97
PU3	422	0.35	-4.00	-0.56	3.44	-4.43	-0.79	3.64

^a Onset absorption wavelength of PI films;

^b $E_{\text{onset}}^{\text{peak}}$: onset potential from cyclic voltammetry vs Ag/AgCl in 0.1 mol/L TBAP/CH₃CN.

^c Based on formula (1) $E_{\text{HOMO}} = (E_{\text{ox/onset}} \text{ vs Ag/AgCl} + 4.43) \text{ eV}$ and (2) $E_{\text{LUMO}} = E_{\text{HOMO}} + E_{\text{g}}$.

^d $E_{\text{g}}^{\text{film}} = 1240/\lambda_{\text{onset}}$.

^e Quantum theoretical calculation of the PUs.

Table S3. Electrochromic properties of PUs.

PU _s	λ^a (nm)	ΔT (%)	Response time ^b		ΔOD^c	Q_d^d (mC cm ⁻²)	CE ^e (cm ² C ⁻¹)
			t_c (s)	t_b (s)			
PU1	804	52	2.9	1.3	0.53	2.67	198
PU2	901	23	6.2	5.4	0.19	2.26	84
PU3	609	34	4.6	2.6	0.31	2.09	148

^a Wavelength of absorption maximum.

^b Time for switching color t_c and bleaching color t_b .

^c Optical density (OD) = $\log[T_{\text{bleached}}/T_{\text{colored}}]$.

^d Q_d is ejected charge.

^e Coloration efficiency (CE) $\eta = \Delta OD / Q_d$.